Liquid Crystals
Publication details, including instructions for authors and subscription information:
http://www.informaworld.com/smpp/title~content=t713926090

High pressure differential thermal analysis of dimer liquid crystals: α, ω-Bis [(4,4'-cyanobiphenylyl) oxy] alkanes

Yoji Maeda[a]; Hidemine Furuya[b]; Akihiro Abe[c]
[a] National Institute of Materials and Chemical Research, Tsukuba, Ibaraki, Japan [b] Department of Polymer Chemistry, Tokyo Institute of Technology, Ookayama, Tokyo, Japan [c] Department of Industrial Chemistry, Tokyo Institute of Polytechnics, Atsugi, Japan

To cite this Article Maeda, Yoji , Furuya, Hidemine and Abe, Akihiro(1996) 'High pressure differential thermal analysis of dimer liquid crystals: α, ω-Bis [(4,4'-cyanobiphenylyl) oxy] alkanes', Liquid Crystals, 21: 3, 365 — 371
To link to this Article: DOI: 10.1080/02678299608032845
URL: http://dx.doi.org/10.1080/02678299608032845

LIQUID CRYSTALS, 1996, VOL. 21, NO. 3, 365–371

High pressure differential thermal analysis of dimer liquid crystals: α, ω-Bis[(4,4′-cyanobiphenylyl)oxy]alkanes

by YOJI MAEDA*
National Institute of Materials and Chemical Research, 1-1 Higashi, Tsukuba,
Ibaraki 305, Japan

HIDEMINE FURUYA
Department of Polymer Chemistry, Tokyo Institute of Technology, Ookayama,
Meguro-ku, Tokyo 152, Japan

and AKIHIRO ABE
Department of Industrial Chemistry, Tokyo Institute of Polytechnics, 1583 Iiyama,
Atsugi 243-02, Japan

(Received 27 February 1996; accepted 4 May 1996)

The phase behaviour of dimer liquid crystals (DLC), α,ω-bis[(4,4′-cyanobiphenylyl)oxy]alkanes (CBA-n with $n=9,10$) has been studied by differential thermal analysis (DTA) over a pressure range from 0·1 to 150 MPa. Both samples exhibit crystal (Cr)↔nematic (N)↔isotropic (I) transitions under all experimental conditions. The slopes of the phase boundary curve $(\mathrm{d}p/\mathrm{d}t)_{\mathrm{tr}}$ were determined from the P_{tr} vs. T_{tr} phase diagram, where the subscript $_{\mathrm{tr}}$ designates $_{\mathrm{CrN}}$ or $_{\mathrm{NI}}$. Both transition temperatures T_{CrN} and T_{NI} were found to increase almost linearly as a function of pressure; CBA-9: $(\mathrm{d}p/\mathrm{d}t)_{\mathrm{CrN}}=3{\cdot}92$, $(\mathrm{d}p/\mathrm{d}t)_{\mathrm{NI}}=2{\cdot}03$; CBA-10: $(\mathrm{d}p/\mathrm{d}t)_{\mathrm{CrN}}=3{\cdot}66$, $(\mathrm{d}p/\mathrm{d}t)_{\mathrm{NI}}=2{\cdot}17$, the units being MPa K^{-1}. As a consequence, the nematic region defined by the interval between the CrN and NI transitions becomes broader as the applied pressure increases. While the transition enthalpies ΔH_{CrN} and the associated entropies ΔS_{CrN} at the CrN transition decrease substantially with increasing pressure, the corresponding quantities at the NI transition remain nearly insensitive to pressure. At atmospheric pressure, the magnitude of ΔH_{NI} amounts to about 10% of ΔH_{CrN} for the given samples. The transition enthalpies and entropies were also estimated from the Clapeyron relation, the volume changes required in this expression being taken from the PVT measurements previously reported. Somewhat larger values were obtained for both ΔH_{tr} and ΔS_{tr} in the latter estimation. The odd–even character with the spacer length n was clearly observed in the aforementioned thermodynamic quantities over the entire pressure range examined.

1. Introduction

Dimer liquid crystals (DLC) such as α,ω-bis[(4,4′-cyanobiphenylyl)oxy]alkanes (CBA-n with $n=9,10$)

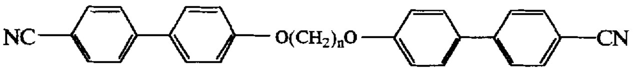

exhibit two well-defined transitions at the crystal–nematic (CrN) and nematic–isotropic (NI) interphases. The odd–even effect has been observed in various thermodynamic quantities at the NI transition as a function of the number of carbon atoms n involved in the spacer [1]. Because of the similarity in their thermodynamic characteristics, including the odd–even effect, DLCs are often regarded as a model for the main chain polymer liquid crystals [2]. In these systems, the orientational order parameter of the mesogenic core axis observed in the vicinity of T_{NI} also oscillates with n, suggesting that the order–disorder transition of the mesogenic core is coupled with the conformational change of the flexible spacer [3–6]. It has been concluded from ^{2}H NMR analysis that the flexible spacer carrying the mesogenic cores on its termini prefers to take more or less extended conformations in the nematic state [4]. Configurational characteristics of chain molecules in the crystalline, liquid crystalline, and isotropic liquid states must manifest themselves in the conformational entropy changes of the system upon phase transition.

CBA-n compounds are known to exhibit appreciable changes in enthalpy and entropy, as well as in the specific volume at the NI transition [7]. The corresponding changes observed for their low molar mass analogues

---

*Author for correspondence.

0267–8292/96 $12·00 © 1996 Taylor & Francis Ltd.

(monomer LCs) are much smaller [8]. Comparison immediately reveals an important role of the spacer in determining the first order character of the transition in the DLC systems. The spatial arrangement of the spacer is somewhat restricted in the nematic state. Upon transition to the isotropic state, such an orientational restriction is removed, and the spacer is allowed to adopt the random coil conformation. This is the origin of the conformational contribution to the thermodynamic quantities which characterize the transition. In fact, it is well known for various semi-flexible polymers that the conformational change at the phase transition constitutes a major contribution to the entropy of fusion, which is an important factor in establishing the melting temperature [9, 10].

In this study, the differential thermal analysis (DTA) of CBA-9 and -10 was performed under pressure (0·1–150 MPa). One of the major interests was to determine the phase boundary curves for both the CrN and NI transitions, which lead to an estimate of the enthalpies of transition on the basis of the Clapeyron relation [11]. It was also interesting to find if the odd–even character of the thermodynamic quantities at the NI transition still holds under high pressure.

2. Experimental

The preparation of CBA-9 and -10 has been described elsewhere [1, 4]. The thermal analysis was carried out using a Perkin-Elmer differential scanning calorimeter II-C (DSC). Transition temperatures were defined at the maxima of the exo- and endo-thermic peaks of the DSC curves. In order to investigate some possible crystallographic modifications of CBA-9 samples, X-ray diffraction measurements were carried out using a Rigaku Diffractometer.

The thermal behaviour of CBA-9 and -10 was examined under hydrostatic pressures up to 200 MPa by using a high pressure DTA apparatus [12] similar to the one previously reported by Takamizawa *et al.* [13]. The sample was fixed onto a platinum holder by giving it a coating with an epoxy adhesive, which at the same time prevented the sample from direct exposure to the pressure fluid (silicone oil). The temperature and the heat of transition were calibrated with an indium standard at given pressures; the accuracy of the observed enthalpy of transition is estimated to be $\pm 10\%$. The DTA measurements were performed by using 3–5 mg samples at a scanning rate of $5\,\mathrm{K\,min^{-1}}$ under given hydrostatic pressures.

3. Results

3.1. *Preliminary studies on polymorphism in the crystalline phase*

A powder sample of CBA-9 prepared by reprecipitation from chloroform solution exhibits two sharp endothermic peaks on heating, corresponding to the CrN and NI transitions. Shown in figure 1 are the DSC curves observed on cooling and subsequent (2nd) heating. Under a given cooling condition ($5\,\mathrm{K\,min^{-1}}$), a metastable crystalline phase ($\mathrm{Cr_l}$) may be formed immediately after the transition from the nematic phase. On the 2nd heating, an endothermic peak appeared at about 401 K and subsequently a sharp exothermic peak at about 402 K, indicating that the melting of $\mathrm{Cr_l}$ is followed by recrystallization to a more stable form $\mathrm{Cr_h}$. Figure 2 indicates the X-ray diffraction diagrams for (*a*) a CBA-9 sample obtained by cooling from the isotropic melt and (*b*) the same sample after heating slowly up to 399 K. By the heat treatment in the immediate vicinity of the melting point, some of the diffraction peaks in figure 2 (*a*) were eliminated to yield figure 2 (*b*). No appreciable changes were observed in the X-ray diagram at lower temperatures ($298 \sim 393$ K). These X-ray observations are consistent with the results of the aforementioned DSC measurements. The fraction of the coexisting $\mathrm{Cr_l}$ phase tends to be suppressed when the cooling rate is reduced. Malpezzi *et al.* [14] reported the results of the crystallographic analysis of CBA-7, concluding that the spacer takes an extended all-*trans*-arrangement. The molecular conformation in the $\mathrm{Cr_h}$ form may be similar to that of CBA-7. The $\mathrm{Cr_h}$ crystal transforms into the nematic state at about 407 K and eventually into the isotropic state at about 445 K as indicated by a large(CrN) and a small(NI) endothermic peak, respectively.

The DTA heating curves for a rapidly cooled CBA-9 sample ($5\,\mathrm{K\,min^{-1}}$) exhibited two peaks in the CrN transition region at all pressures: a small endothermic peak corresponding to the fusion of the relatively unstable $\mathrm{Cr_l}$ crystal and a large endothermic peak due to melting of the regular $\mathrm{Cr_h}$ crystal. A less distinct endothermic peak appearing at a higher temperature corresponds to the NI transition. The DTA thermograms were found to be similar to those observed at atmospheric pressure (figure 1) except for the omission of the exothermic trough associated with the formation of the $\mathrm{Cr_h}$ crystal involved in the $\mathrm{Cr_l} \rightarrow \mathrm{Cr_h}$ transformation. This difference probably arises from the lower sensitivity of the high pressure DTA apparatus relative to the commercial DSC equipment. In brief, the general features of the thermal behaviour of CBA-9 remain essentially unaltered over a wide range of applied pressure. The T_{tr} vs. P_{tr} phase diagram obtained during a heating process yielded first order polynomials such as

$$\begin{aligned} \mathrm{Cr_l} \rightarrow \mathrm{Cr_h}&: \quad t = 402{\cdot}4 + 0{\cdot}179_5 p \\ \mathrm{Cr_h} \rightarrow \mathrm{N}&: \quad t = 408{\cdot}9 + 0{\cdot}247_4 p \qquad (1) \\ \mathrm{N} \rightarrow \mathrm{I}&: \quad t = 445{\cdot}2 + 0{\cdot}474_7 p \end{aligned}$$

The coexisting $\mathrm{Cr_l}$ crystal, which melts at a lower temperature, was found to transform into the stable $\mathrm{Cr_h}$

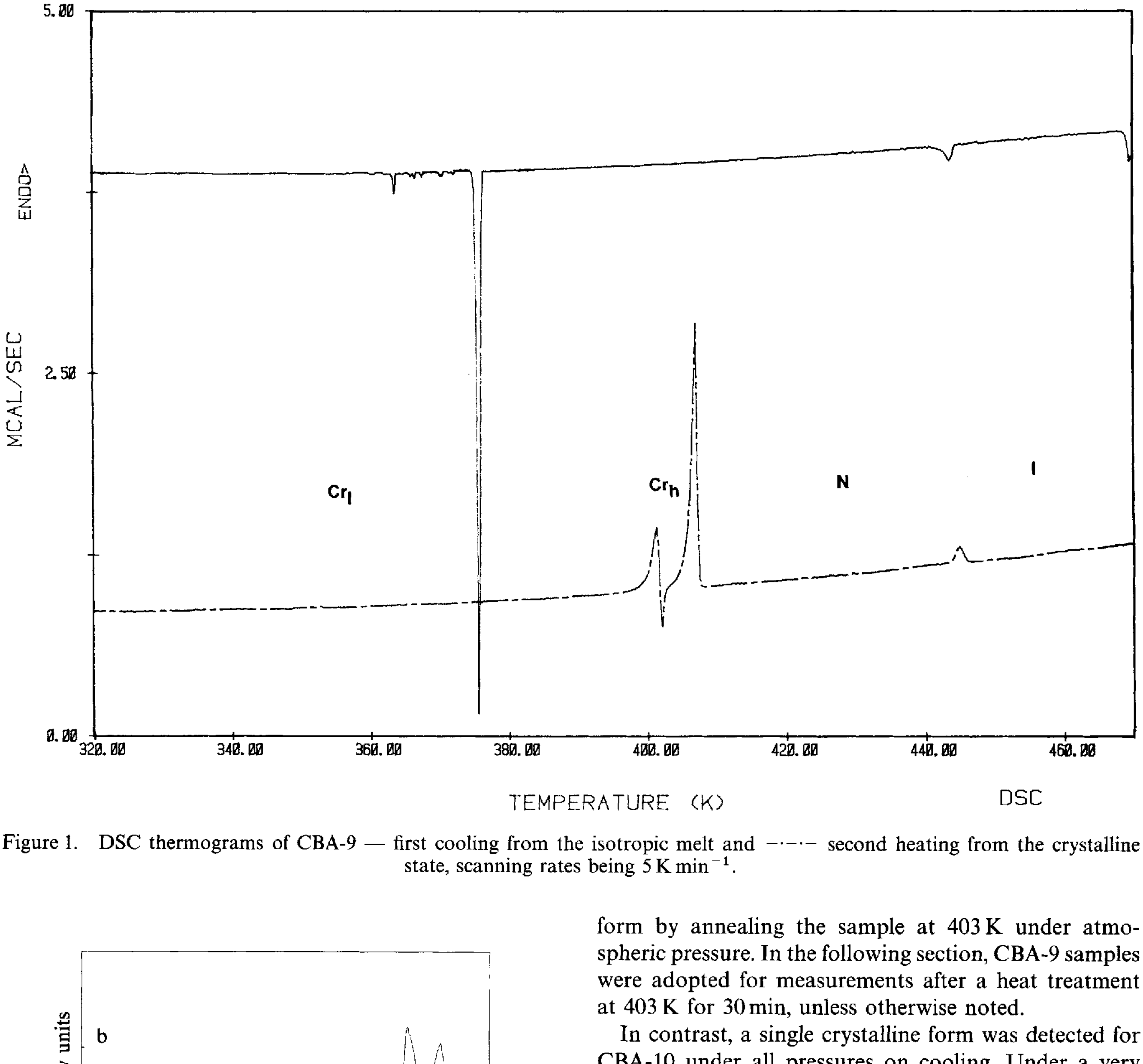

Figure 1. DSC thermograms of CBA-9 — first cooling from the isotropic melt and –·–·– second heating from the crystalline state, scanning rates being 5 K min^{-1}.

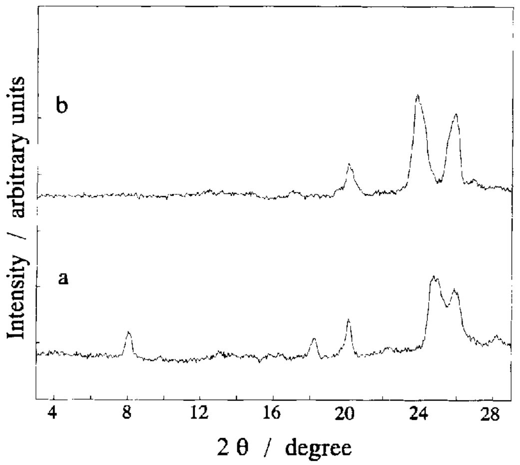

Figure 2. X-ray diffraction patterns of CBA-9: (*a*) rapidly cooled (5 K min^{-1}) from the isotropic melt, measured at room temperature and (*b*) the same sample after heating slowly to 399 K.

form by annealing the sample at 403 K under atmospheric pressure. In the following section, CBA-9 samples were adopted for measurements after a heat treatment at 403 K for 30 min, unless otherwise noted.

In contrast, a single crystalline form was detected for CBA-10 under all pressures on cooling. Under a very high pressure (~200 MPa), however, a somewhat unusual DTA behaviour was observed. When the CBA-10 sample was cooled from the nematic state at 200 MPa, a very small exothermic peak appeared at lower temperatures. The degree of supercooling associated with the N→Cr transition also diminished from a common value (~40 K) to ~20 K under this condition. This may suggest the possible occurrence of polymorphism under high pressure. In fact, such samples exhibit an extra shoulder on the CrN transition peak in the DTA diagram. The present report therefore excludes the results obtained at pressures higher than 150 MPa. The investigation of the thermal behaviour in the region $P > 150$ MPa was beyond the scope of the present study.

Table 1. Comparison of DSC and DTA data on the CrN and NI transitions of CBA-9 and -10 at atmospheric pressure.

	CrN transition			N-I transition		
Method	$T_{\rm CrN}$ /K	$\Delta H_{\rm CrN}$ /kJ mol^{-1}	$\Delta S_{\rm CrN}$ /J mol^{-1} K^{-1}	$T_{\rm NI}$ /K	$\Delta H_{\rm NI}$ /kJmol^{-1}	$\Delta S_{\rm NI}$ /J mol^{-1} K^{-1}
			CBA-9			
DSC	406·8	47·0	115·5	445·5	3·75	8·4
DTA (0·1 MPa)	408·3	43·5	106·5	444·0	3·6	8·1
			CBA-10			
DSC	438·7	53·1	121·0	457·6	8·2	18·0
DTA (0·1 MPa)	440·6	50·3	114·2	456·7	7·3	16·0

3.2. *Comparison of phase transition behaviour of CBA-9 and -10*

In table 1, thermodynamic data obtained by DSC are compared with those obtained by DTA at 0·1 MPa. The CBA-9 and -10 samples used in these measurements exhibited a typical transition pattern consisting of a set of major and minor peaks corresponding to the CrN and NI transitions, respectively. The results derived by the two different methods agree reasonably well within the precision of the apparatus used. In accordance with previous observations [1, 3, 4], a distinct odd–even effect with the spacer length can be seen in the transition entropy $\Delta S_{\rm NI}$: the magnitude of $\Delta S_{\rm NI}$ for CBA-9 is about one half that of CBA-10.

Typical examples of the DTA (heating) curves obtained at a higher hydrostatic pressure (100 MPa) are illustrated for CBA-9 and -10 in figure 3. General features observed by DSC under atmospheric pressure are mostly retained at higher pressures. The $T_{\rm tr}$ vs. $P_{\rm tr}$ plots are shown in figure 4. For both samples, the CrN and NI phase transition curves can be expressed in first order polynomial forms such as

$$\begin{array}{lll} \text{CBA-9} & \text{Cr}_{\rm h}\rightarrow\text{N:} & t=408{\cdot}3+0{\cdot}255_4 p \\ & \text{N}\rightarrow\text{I:} & t=444{\cdot}0+0{\cdot}491_8 p \end{array} \qquad (2)$$

$$\begin{array}{lll} \text{CBA-10} & \text{Cr}\rightarrow\text{N:} & t=440{\cdot}6+0{\cdot}273_4 p \\ & \text{N}\rightarrow\text{I:} & t=456{\cdot}8+0{\cdot}461_2 p \end{array} \qquad (3)$$

As indicated in figure 4, the nematic range defined by the temperature interval between the CrN and NI

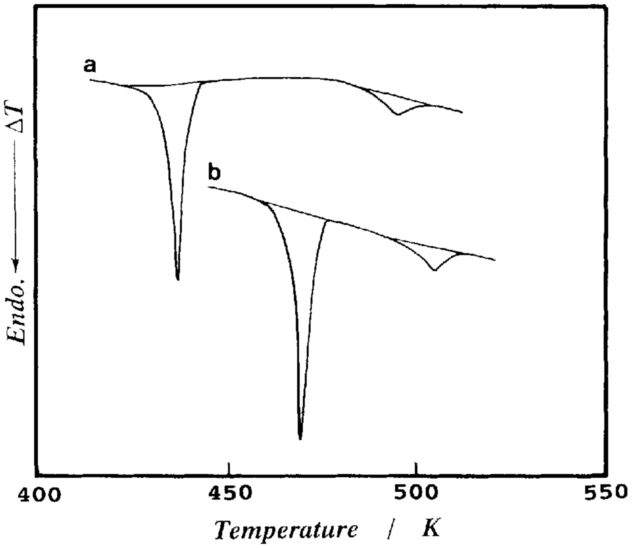

Figure 3. High pressure DTA curves of (*a*) CBA-9 (annealed) and (*b*) CBA-10 samples at 100 MPa. Heating rate 5 K min^{-1}.

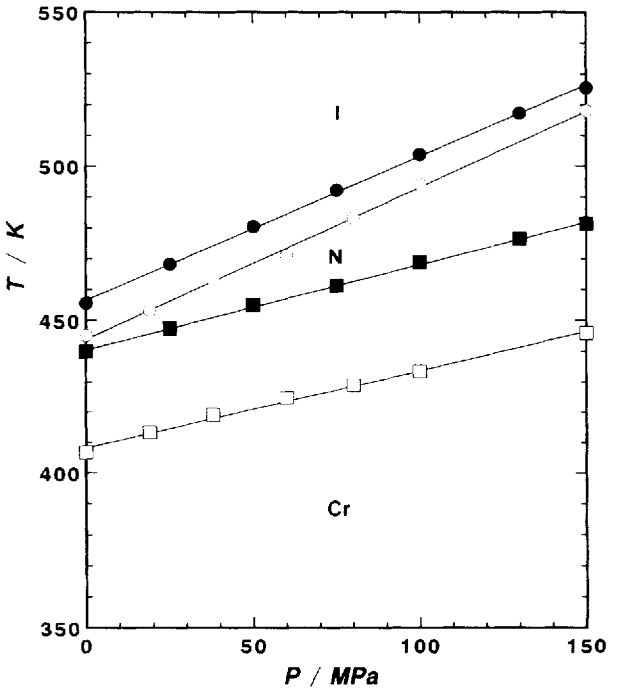

Figure 4. Variation of transition temperatures $T_{\rm tr}$ as a function of pressure P during heating: □($T_{\rm CrN}$), ○($T_{\rm NI}$) for CBA-9 (annealed) and ■($T_{\rm CrN}$), ●($T_{\rm NI}$) for CBA-10.

transitions becomes somewhat broader with increasing pressure. This phenomenon is widely known for conventional liquid crystals [15]. The T_{tr} vs. P_{tr} relation associated with the $Cr_h \rightarrow N$ transition of CBA-9 (equation (2)) is consistent with that shown in equation (1), suggesting that the transition temperatures are not affected by the coexisting C_l phase.

Variations of the transition enthalpies ΔH_{NI} and ΔH_{CrN} with pressure are illustrated for both CBA-9 and -10 in figure 5 (*a*), where the experimental data obtained by DSC under atmospheric pressure are also included. At $P=0{\cdot}1$ MPa, the ratio $\Delta H_{NI}/\Delta H_{CrN}$ amounts to 0·08 and 0·14, respectively, for CBA-9 and -10. While ΔH_{CrN} decreases substantially (13 ~ 18%) as the pressure increases, ΔH_{NI} remains nearly constant over the entire range of pressure. The transition entropies ΔS_{NI} and ΔS_{CrN} estimated concurrently are plotted against pressure in figure 5 (*b*). General trends are similar between figures 5 (*a*) and 5 (*b*). The ΔS_{NI} value of CBA-9 is about one half that of CBA-10 at all pressures, indicating that the odd–even oscillation of ΔS_{NI} with the spacer length remains unaltered over a wide range of pressure.

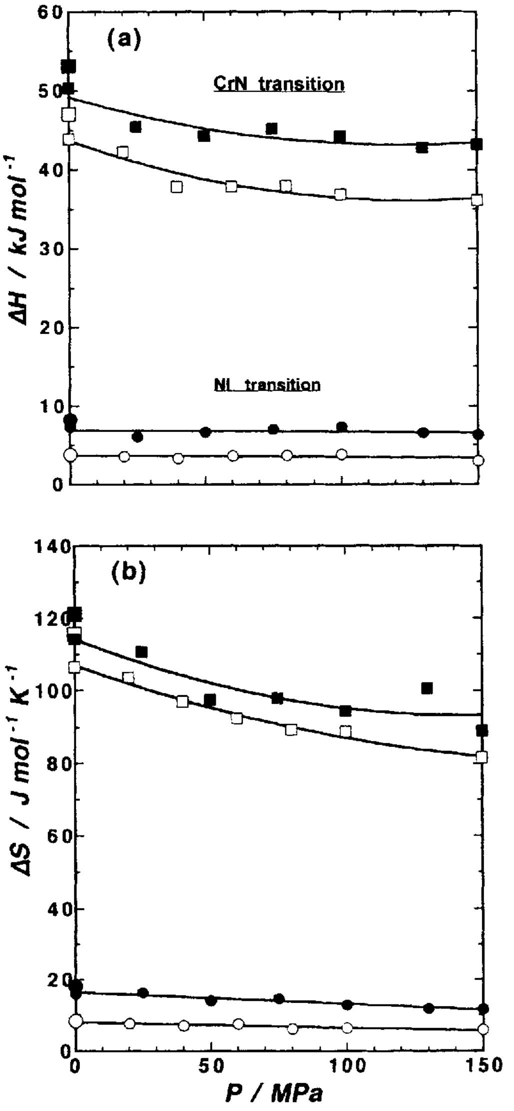

Figure 5. Pressure dependence of (*a*) transition enthalpies (ΔH_{CrN}, ΔH_{NI}) and (*b*) entropies (ΔS_{CrN}, ΔS_{NI}) of CBA-9 and -10 samples; the experimental data obtained by DSC under atmospheric pressure are also included. For symbols, see legend for figure 4.

4. Discussion

The results obtained by DSC may be favourably compared with those of DTA at 0·1 MPa (table 1). The transition temperatures T_{CrN} and T_{NI} are in agreement within 2 K. The enthalpies ΔH_{CrN} were somewhat underestimated in the DTA measurement (5–10%), and accordingly the associated entropies ΔS_{CrN} are also lower. Another set of DSC data is available on the same sample from the work of Abe *et al.* [7]: while the transition temperatures are in agreement for given DLCs, the enthalpies of CBA-10 are slightly higher (5–10%) than those of the present measurements. The enthalpy changes at the phase transition can be alternatively estimated with the aid of the Clapeyron relation [11]

$$\Delta H_{tr} = T_{tr} \Delta V_{tr} \mathrm{d}p/\mathrm{d}t \qquad (4)$$

where the transition volumes ΔV_{tr} are available from *PVT* measurements [7]. The slope of the phase boundary curve $\mathrm{d}p/\mathrm{d}t$ can be estimated from the relation (equations (2) and (3)) derived from the T_{tr}–P_{tr} plot (figure 4); CBA-9: $(\mathrm{d}p/\mathrm{d}t)_{CrN}=3{\cdot}92$, $(\mathrm{d}p/\mathrm{d}t)_{NI}=2{\cdot}03$; CBA-10: $(\mathrm{d}p/\mathrm{d}t)_{CrN}=3{\cdot}66$, $(\mathrm{d}p/\mathrm{d}t)_{NI}=2{\cdot}17$, the units being MPa K^{-1}. The transition enthalpies and entropies estimated from equation (4) at $P=0{\cdot}1$, 50, and 100 MPa are summarized in table 2. For comparison, the corresponding values obtained directly by DTA are indicated in parentheses; they are taken from the best-fit curves shown in figures 5 (*a*) and 5 (*b*). Both ΔH_{tr} and ΔS_{tr} calculated by using the Clapeyron relation substantially exceed those directly determined by DSC or DTA. The difference between the two approaches, i.e. the use of the Clapeyron relation, equation (4), and the direct determination by DSC or DTA method, is apparent. While the heats estimated by the former method are a measure of the discontinuity of the first order transition at a given temperature, those from the calorimetric measurements may include some additional contribution due to pre- and post-transitional phenomena occuring in the immediate vicinity of the transition. In addition, some difficulty is inevitably involved in selecting a baseline in the DSC method. The transition entropies found for CBA-*n* are appreciably larger than those estimated for related low molar mass liquid crystals such

Table 2. Transition enthalpies ΔH_{tr} and entropies ΔS_{tr} estimated from the Clapeyron relation.

	CrN transition				NI transition			
P /MPa	T_{CrN} /K	ΔV_{CrN}[a] /cm^3 mol^{-1}	ΔH_{CrN}[b] /kJ mol^{-1}	ΔS_{CrN}[b] /J mol^{-1} K^{-1}	T_{NI} /K	ΔV_{NI}[a] /cm^3 mol^{-1}	ΔH_{NI}[b] /kJ mol^{-1}	ΔS_{NI}[b] /J mol^{-1} K^{-1}
CBA-9								
0·1	408·3	37·5	60·0	147·0	444·0	7·5	6·8	15·3
			(43·5)	(106·5)			(3·6)	(8·1)
50	422·2	31·3	51·8	122·7	469·7	5·4	5·1	10·9
			(40·9)	(96·9)			(3·4)	(7·2)
100	433·7	27·3	46·4	107·0	493·1	5·2	5·2	10·5
			(38·2)	(88·1)			(3·2)	(6·5)
CBA-10								
0·1	440·6	39·3	63·4	143·8	456·7	9·4	9·3	20·4
			(50·3)	(114·2)			(7·3)	(16·0)
50	454·6	33·6	55·9	123·0	480·6	8·5	8·9	18·5
			(44·3)	(97·4)			(6·7)	(13·9)
100	469·3	30·7	52·7	112·3	504·6	7·5	8·2	16·3
			(44·2)	(94·2)			(7·2)	(14·3)

[a] Taken from ref. [7].

[b] Values in parentheses are those obtained by DTA.

as 4′-*n*-alkyl-4-cyanobiphenyls or 4′-*n*-alkoxy-4-cyanobiphenyls, for which Orwoll *et al.* [8] reported entropy changes in the range 0·2–0·8 J mol^{-1} K^{-1}. It has been concluded from the ^{2}H NMR and *PVT* analysis that the conformation of the flexible spacer is largely responsible for such an enhancement of transition entropies [16]. A somewhat contradictory model implying an appreciably lower estimate of the conformational entropy has been presented by Ferrarini *et al.* [17] from their theoretical investigation on the dimer LC system. In treating the transitional properties of dimers or any related main chain LCs including polymers, however, the contribution to the entropy arising from the volume change at the NI transition must also be taken into account. The ΔV_{NI} values for the dimer [7] and the polymer [18] are reported to be substantially larger than those observed for conventional monomer LCs [8].

The enthalpy and entropy changes at the NI transition were previously estimated by using the $(\mathrm{d}p/\mathrm{d}t)_{\mathrm{NI}}$ values obtained from *PVT* measurements; CBA-9: $(\mathrm{d}p/\mathrm{d}t)_{\mathrm{NI}}=$ 2·00; CBA-10: $(\mathrm{d}p/\mathrm{d}t)_{\mathrm{NI}}=2{\cdot}35$, the units being MPa K^{-1}. As shown by comparison, the agreement is satisfactory between the two independent measurements, DTA and *PVT*. Zoller *et al.* [18] also found a reasonably good agreement for the $(\mathrm{d}p/\mathrm{d}t)_{\mathrm{CrN}}$ values ($2\sim5$ MPa K^{-1}) between the *PVT* and high pressure DTA methods in their study on a series of main chain azomethine polymers. The values of $(\mathrm{d}p/\mathrm{d}t)_{\mathrm{NI}}$ obtained above for DLCs are nearly equivalent or slightly smaller than those reported for related low molar mass LCs such as *n*CB (2·4–3·0) and *n*OCB (2·1–3·0) [8].

In the aforementioned *PVT* measurements on DLCs [7], the slopes of the phase boundary curve $(\mathrm{d}p/\mathrm{d}t)_{\mathrm{CrN}}$ could not be estimated with a reasonable accuracy for the CrN transition. Since DTA gives the transition temperature T_{CrN} as an endothermic peak, the slopes of the T_{tr}–P_{tr} relation can be more easily estimated (cf. figure 3). Combined use of the $(\mathrm{d}p/\mathrm{d}t)_{\mathrm{CrN}}$ value thus obtained with the volume change ΔV_{CrN} previously determined leads to an estimate of ΔH_{CrN} and ΔS_{CrN} as given in table 2. In previous work [7], the transition entropies at constant volume $(\Delta S_{\mathrm{CrN}})_{\mathrm{v}}$ were estimated on the basis of the DSC data. Adoption of ΔS_{CrN} values obtained at 0·1 MPa from the Clapeyron relation (table 2) raises the $(\Delta S_{\mathrm{CrN}})_{\mathrm{v}}$ values by about 10–20%. The significance of such an entropy separation has been discussed elsewhere [16, 19].

In this work, the high-pressure DTA method was shown to be useful in estimating accurate values of $(\mathrm{d}p/\mathrm{d}t)_{\mathrm{CrN}}$, which sometimes elude determination from *PVT* measurements. Studies of a homologous series of CBA-*n*, including trimer LCs, are in progress by employing the methodology thus established.

We thank Dr. S. Y. Nam for preparation of CBA-*n* samples (at the time of his residence at Tokyo Institute of Technology).

References

[1] Emsley, J. W., Luckhurst, G. R., Shilstone, G. N., and Sage, I., 1984, *Mol. Cryst. liq. Cryst. Lett.*, **102**, 223.

[2] Stroganou, L., 1993, *Liquid Crystalline and Mesomorphic Polymers*, edited by V. P. Shibaev and L. Lam (Springer-Verlag).

[3] (*a*) Emsley, J. W., Heaton, N. J., Luckhurst, G. R.,

and SHILSTONE, G. N., 1988, *Mol. Phys.*, **64,** 377; (*b*) CHEUNG, S. T. W., and EMSLEY, J. W., 1993, *Liq. Cryst.*, **13,** 265.

[4] (*a*) ABE, A., and FURUYA, H., 1989, *Macromolecules*, **22,** 2982; (*b*) ABE, A., SHIMIZU, R. N., and FURUYA, H., 1994, *Ordering in Macromolecular Systems*, edited by A. Teramoto *et al.* (Springer-Verlag), p. 139.

[5] (*a*) TORIUMI, H., FURUYA, H., and ABE, A., 1985, *Polym. J.*, **17,** 895; (*b*) ABE, A., FURUYA, H., and YOON, D. Y., 1988, *Mol. Cryst. liq. Cryst.*, **159,** 151; (*c*) ABE, A., and FURUYA, H., 1988, *Polym. Bull.*, **19,** 403; **20,** 467.

[6] (*a*) FURUYA, H., DRIES, T., FUHRMANN, K., ABE, A., BALLAUFF, M., and FISCHER, E. W., 1990, *Macromolecules*, **23,** 4122; (*b*) FURUYA, H., ABE, A., FUHRMANN, K., BALLAUFF, M., and FISCHER, E. W., 1991, *ibid*, **24,** 299.

[7] ABE, A., and NAM, S. Y., 1995, *Macromolecules*, **28,** 90.

[8] ORWOLL, R. A., SULLIVAN, V. J., and CAMPBELL, G. C., 1987, *Mol. Cryst. liq. Cryst.*, **149,** 121.

[9] MANDELKERN, L., 1964, *Crystallization of Polymers* (New York: McGraw-Hill).

[10] ABE, A., 1980, *Macromolecules*, **13,** 546.

[11] CLAPEYRON, E., 1961, *Thermodynamics*, edited by K. S. Pitzer and L. Brewer (New York: McGraw-Hill).

[12] (*a*) MAEDA, Y., and KANETSUNA, H., 1985, *Bull. Res. Inst. Polym. Text.*, **149,** 119; (*b*) MAEDA, Y., 1990, *Thermochim. Acta*, **163,** 211.

[13] TAKAMIZAWA, K., NAGAO, Y., IRII, D., and URABE, Y., 1985, *Thermochim. Acta*, **88,** 205.

[14] MALPEZZI, L., BRUCKNER, S., GALBIATI, E., and LUCKHURST, G. R., 1991, *Mol. Cryst. liq. Cryst.*, **195,** 179.

[15] (*a*) SPRATTE, W., and SCHNEIDER, G. M., 1976, *Ber. Bunsenges. phys. Chem.*, **80,** 886; KUSS, E., 1978, *Mol. Cryst. liq. Cryst.*, **47,** 71.

[16] ABE, A., FURUYA, H., SHIMIZU, R. N., and NAM, S. Y., 1995, *Macromolecules*, **28,** 96.

[17] FERRARINI, A., LUCKHURST, G. R., NORDIO, P. L., and ROSKILLY, S. J., 1994, *J. chem. Phys.*, **100,** 1460.

[18] FAKHREDDINE, Y. A., and ZOLLER, P., 1994, *J. Polym. Sci., B, Polym. Phys.*, **32,** 2445.

[19] (*a*) ROBERTSON, R. E., 1969, *Macromolecules*, **2,** 250; (*b*) WUNDERLICH, B., and CZORNYJ, G., 1977, *ibid*, **10,** 906; (*c*) MILLER, A. A., 1979, *ibid*, **12,** 651; (*d*) BLEHA, T., 1985, *Polymer*, **26,** 1638.